

RSC Advances



This is an *Accepted Manuscript*, which has been through the Royal Society of Chemistry peer review process and has been accepted for publication.

Accepted Manuscripts are published online shortly after acceptance, before technical editing, formatting and proof reading. Using this free service, authors can make their results available to the community, in citable form, before we publish the edited article. This *Accepted Manuscript* will be replaced by the edited, formatted and paginated article as soon as this is available.

You can find more information about *Accepted Manuscripts* in the [Information for Authors](#).

Please note that technical editing may introduce minor changes to the text and/or graphics, which may alter content. The journal's standard [Terms & Conditions](#) and the [Ethical guidelines](#) still apply. In no event shall the Royal Society of Chemistry be held responsible for any errors or omissions in this *Accepted Manuscript* or any consequences arising from the use of any information it contains.

1 **DTX-loaded star-shaped TAPP-PLA-*b*-TPGS nanoparticles for cancer chemical and**
2 **photodynamic combination therapy**

3

4 Teng Wang^{a,b,1}, Dunwan Zhu^{c,1}, Gan Liu^b, Wei Tao^b, Wei Cao^b, Linhua Zhang^c, Lijun Wang^b, Hongbo
5 Chen^b, Lin Mei^b, Laiqiang Huang^{a,b,*}, Xiaowei Zeng^{a,b,*}

6

7 ^a *Department of Chemistry, Tsinghua University, Beijing 100084, P.R. China*

8 ^b *The Shenzhen Key Lab of Gene and Antibody Therapy, and Division of Life and Health Sciences,*
9 *Graduate School at Shenzhen, Tsinghua University, Shenzhen 518055, P.R. China*

10 ^c *Institute of Biomedical Engineering, Chinese Academy of Medical Sciences & Peking Union*
11 *Medical College, Tianjin Key Laboratory of Biomedical Materials, Tianjin 300192, P.R. China*

12

13

14

15 ¹ These authors contributed equally to this work.

16 *Corresponding author. Tel./Fax: +86 75526036736.

17 *E-mail address:* zeng.xiaowei@sz.tsinghua.edu.cn (X. Zeng)

18 *Corresponding author. Tel./Fax: +86 75526036052.

19 *E-mail address:* huanglq@sz.tsinghua.edu.cn (L. Huang)

20

21

22

1 Abstract

2 A novel multifunctional material consisting of a four-armed star-shaped porphyrin-cored
3 poly(lactide)-*b*-D- α -tocopheryl polyethylene glycol 1000 succinate amphiphilic copolymer
4 (TAPP-PLA-*b*-TPGS) was synthesized through an arm-first approach and was characterized by ¹H
5 NMR and gel permeation chromatography (GPC). This porphyrin-functionalized material has
6 potential applications in both drug-delivery systems and photodynamic therapy (PDT). Docetaxel
7 (DTX)-loaded or Coumarin 6-loaded nanoparticles (NPs) were prepared by a modified
8 nanoprecipitation technique. The resulting NPs were characterized through determination of their
9 size and size distribution data, surface charge and surface morphology, drug loading content, drug
10 encapsulation efficiency, as well as differential scanning calorimetry (DSC) experiments. In drug
11 release assays, the DTX-loaded NPs showed excellent pH-dependent drug-release behavior. The NPs
12 were also found to generate singlet oxygen (¹O₂) species and exhibit significant phototoxicity in
13 HeLa cervical cancer cells after irradiation with light of 660 nm wavelength. The drug-loaded NPs
14 demonstrated superior performance compared to the commercial drug, Taxotere[®], which is likely due
15 to synergistic effects between phototherapy and chemotherapy in the destruction of HeLa cells. This
16 novel functionalized drug-delivery system shows considerable potential in providing a new
17 multi-modality treatment approach for cancer.

18 **Keywords:** Drug-delivery system; Star-shaped copolymer; Multimodality treatment; Nanoparticles;
19 Photodynamic therapy

1 Introduction

2 Cervical cancer is not only the fourth most common type of cancer but also the fourth most
3 common cause of cancer death among women worldwide. Studies show that nearly 530,000 women
4 were diagnosed with cervical cancer in 2012, with 85% of them in developing countries.^{1,2} The
5 current clinical approaches for cervical cancer treatment are still limited to surgical resection,
6 radiation and consolidation chemotherapy, which can be nonspecific and can have several side
7 effects.³ Over the past two decades, the semi-synthetic taxane analog, docetaxel, has been widely
8 used in the treatment of cervical cancer. Docetaxel is an anti-mitotic chemotherapy medication which
9 works by inducing tubulin polymerization.⁴ However, because of its extremely low water solubility,
10 the commercial drug form of docetaxel is dissolved in high concentrations of Tween 80 (polysorbate
11 80), which could lead to various side effects such as hypersensitivity reactions, gastrointestinal
12 problems, cardiotoxicity and neurotoxicity.⁵

13 Recently, a new treatment option for cancer has been developed based on photodynamic therapy
14 (PDT). PDT is a form of phototherapy in which irradiation with light of a specific wavelength light
15 activates photosensitizers (PS), which then generate the powerful reactive oxygen species (ROS).
16 ROS are capable of destroying the cancer cells by damaging the biomacromolecules and organelles
17 within the cells.⁶⁻⁸ Unlike other therapy, PDT is a precisely targeted treatment which is controlled by
18 selecting appropriate wavelength light.^{6,9,10} Moreover, PDT can be used to treat the same site
19 repeatedly, and is non-invasive. However, due to the hydrophobicity of most photosensitizers, they
20 show unsatisfactory biodistribution properties and skin toxicity.¹¹

21 Nanomedicines, especially the biodegradable polymeric nanoparticles (NPs), are commonly
22 used as drug delivery systems,¹²⁻¹⁴ and may overcome the above disadvantages. The amphiphilic

1 biodegradable block copolymers have the ability to encapsulate various poorly soluble agents and
2 form micelles through self-assembly due to hydrophobic-lipophilic interactions.^{3,15-17} Polylactic
3 acid (PLA), a biodegradable thermoplastic aliphatic polyester, is being increasingly explored in
4 medical applications.^{18,19} As the decomposition product of PLA is the harmless lactic acid, PLA can
5 be safely used as medical implants.²⁰ However, as PLA is extremely hydrophobic, the drug carriers
6 based on PLA are rapidly captured by the reticuloendothelial system (RES) when injected into the
7 blood stream.^{21,22} This can be solved by conjugating D- α -tocopheryl polyethylene glycol 1000
8 succinate (vitamin E TPGS or simply TPGS) to PLA to lower its hydrophobicity. TPGS, a
9 water-soluble derivative of natural vitamin E, is prepared by the esterification of vitamin E succinate
10 with PEG 1000.²³ It has been reported that TPGS can serve as an emulsifier in NPs. TPGS also
11 improves the solubility, permeability and stability of the formulated drug, and increases its cellular
12 uptake.²³⁻²⁶ Moreover, TPGS has been shown to reduce multi-drug resistance (MDR) of tumor cells
13 through P-glycoprotein inhibition,²⁷⁻²⁹ and it has been approved by the U.S. Food and Drug
14 Administration (FDA) in drug delivery.²⁵ The preparation techniques of polymeric nanoparticles
15 include nanoprecipitation, dialysis, solvent evaporation and multiple emulsions.^{3,30,31}

16 Star-shaped block copolymers have recently attracted considerable attention owing to their
17 unique properties and applicability in nanomedicine development.³² The drug loaded star-shaped
18 NPs have a lower solution viscosity, smaller hydrodynamic radius, higher drug loading content (LC)
19 and higher drug encapsulation efficiency (EE) than the drug loaded linear NPs with the same
20 molecular weight and composition.^{33,34} One type of classic photosensitizer is porphyrin derivative,
21 which has the excellent biocompatible porphyrin moiety and is widely used in PDT, such as
22 Photofrin had been approved for the prophylactic treatment of bladder cancer in 1993 in Canada.^{6,9}

1 5,10,15,20-tetrakis(4-aminophenyl)-21H,23H-porphine (TAPP) is a porphyrin-based photosensitizer.
2 And it is a desirable core for synthesizing star-shaped amphiphilic copolymers, because it has
3 multiple functional groups at its periphery.^{35,36} For example, poly(3-caprolactone)-
4 poly(ethyleneglycol) diblock copolymer with TAPP as core was synthesized for use in
5 PDT-functionalized drug delivery system.¹¹ Therefore, TAPP-functionalized star-shaped copolymers
6 would have great potential in nanomedicine and PDT for cancer therapy.

7 In the present study, we have attempted to create efficient docetaxel nanocarriers for PDT based
8 cervical cancer treatment in the form of a novel amphiphilic star-shaped block copolymer of TAPP-
9 centered, 4-armed star PLA-*b*-TPGS. The drug loading content, drug encapsulation efficiency, and
10 singlet oxygen production ability of the drug-loaded star-shaped TAPP-PLA-*b*-TPGS NPs were
11 evaluated, and their cytotoxicity and phototoxicity were also investigated in vitro.

12 2. Materials and Methods

13 2.1 Materials

14 D- α -tocopheryl polyethylene glycol 1000 succinate (TPGS, C₃₃O₅H₅₄(CH₂CH₂O)₂₃) was
15 purchased from Sigma-Aldrich (St Louis, MO, USA). 5,10,15,20-Tetrakis(4-aminophenyl)porphyrin
16 (TAPP, C₄₄H₃₄N₈) was obtained from Tokyo Chemical Industry (TCI, Tokyo, Japan). D,L-lactide
17 (LA), acetonitrile and methanol (HPLC grade), stannous octoate (Sn(Oct)₂), coumarin-6,
18 1,3-diisopropylcarbodiimide (DCC), N-hydroxysuccinimide (NHS), 4-(dimethylamino) pyridine
19 (DMAP), 1,3-diphenylisobenzofuran (DPBF) and
20 3-(4,5-dimethylthiazol-2-yl)-2,5-diphenyltetrazolium bromide (MTT) were purchased from
21 Sigma-Aldrich (St Louis, MO, USA). Docetaxel (DTX) was provided by Shanghai Jinhe Bio-tech
22 Co., Ltd. (Shanghai, PR China). All the commercial chemicals that were used in this study were of

1 the highest grade. Anti- α -tubulin was purchased from Abcam (Cambridge, UK) and A FITC
2 conjugated goat anti-rabbit IgG antibody was purchased from Santa Cruz (Texas, USA).
3 4',6-Diamidino-2-phenylindole dihydrochloride (DAPI) was purchased from Sangon Biotech
4 (Shanghai, China). Human cervix carcinoma cell line HeLa cells were grown in our lab.

5 *2.2 Synthesis of star-shaped copolymer TAPP-PLA-b-TPGS*

6 The star-shaped block copolymer TAPP-PLA-*b*-TPGS was synthesized as described in previous
7 reports.^{32,37} The synthetic route of the TAPP-PLA-*b*-TPGS star-shaped polymer is summarized in
8 scheme 1.

9 *2.2.1 Synthesis of linear copolymer PLA-b-TPGS*

10 Initiator TPGS ($M_n=1500$, 1.50 g, 1.0 mmol), D,L-lactide ($M_n=144$, 8.6 g, 60 mmol) and catalyst
11 Sn(Oct)₂ (0.024 g, 0.1 mol% of monomer) were added to a glass tube which was connected to a
12 vacuum system. In order to remove air and moisture, the system was evacuated and refilled with
13 inert argon three times. The evacuated tube was then sealed, and the ring opening polymerization
14 reaction was allowed to proceed for 10 h at 150 °C. After the reaction, the tube was cooled to room
15 temperature. The product was dissolved in dichloromethane. Then the polymer was precipitated in
16 excess cold anhydrous ether, washed with a solvent mixture of ether and methanol. The final product,
17 PLA-*b*-TPGS, was placed in a vacuum drying oven and dried at 40 °C for 24 h.

18 *2.2.2 Synthesis of carboxyl-terminated TPGS-b-PLA-COOH*

19 PLA-*b*-TPGS ($M_n \approx 10100$, 5.00 g, 0.5 mmol), succinic anhydride (200 mg, 2.0 mmol), DMAP
20 (122 mg, 5.0 mmol) and TEA (101 mg, 1.0 mmol) were dissolved in anhydrous dioxane (50 ml) and
21 stirred under inert argon at room temperature for 24 h. The solvent was completely removed by
22 vacuum distillation in a rotary evaporator. The residue was re-dissolved in dichloromethane and

1 washed with 10% HCl (3 × 30 mL) and brine (3 × 30 mL). The organic layer was then dried with
2 anhydrous MgSO₄ overnight, filtered, and precipitated in cold diethyl ether. The precipitated product,
3 carboxyl-terminated TPGS-PLA-*b*-COOH, was dried under vacuum at 40 °C for 24 h.

4 *2.2.3 Synthesis of star-shaped copolymer TAPP-PLA-*b*-TPGS*

5 TPGS-*b*-PLA-COOH (2.0 g, 0.2 mmol), NHS (34.5 mg, 0.3 mmol), DCC (41.3 mg, 0.2 mmol),
6 and DMAP (36.6 mg, 0.3 mmol) were dissolved in anhydrous dichloromethane (25 ml) and stirred
7 under inert argon at room temperature for 24 h. Then TAPP (45 mg, 0.0625 mmol) was added to the
8 mixture, and stirring was continued under inert argon at room temperature for another 24 h. The
9 reaction mixture was then filtered and precipitated in cold anhydrous ether. The precipitate was dried
10 under vacuum at 40 °C for 24 h and re-dissolved in acetone. As the final purification step, the
11 acetone solution was placed in a dialysis membrane bag (MW cut-off: 10,000 Da) and immersed in
12 500 ml acetone for 48 h to remove unreacted TPGS-*b*-PLA-COOH and other impurities. The
13 solution was then evaporated in a rotary evaporator, and the resulting solid pure product was dried at
14 40 °C in a vacuum drying oven.

15 *2.3 Characterization of polymers*

16 The structures of copolymers PLA-*b*-TPGS and TAPP-PLA-*b*-TPGS were confirmed by ¹H
17 NMR (Bruker AMX 500) with CDCl₃ as solvent. Molecular weights of the copolymers were
18 measured by GPC (Waters GPC analysis system with RI-G1362A refractive index detector, Waters
19 Corp., Milford, MA, USA) with THF as the eluent at the flow rate of 1 mL/min. Molecular weight
20 and polydispersity index (PDI) were evaluated using standard polystyrene samples.

21 *2.4 Preparation of NPS with and without DTX loading, and with coumarin-6 loading*

22 DTX-loaded TAPP-PLA-*b*-TPGS and PLA-*b*-TPGS NPs were prepared by a nanoprecipitation

1 method using an acetone/water system, as reported previously.^{29,38} Briefly, 100 mg copolymer and
2 10 mg DTX were fully dissolved in 8 mL acetone. The mixture was then slowly added using a
3 syringe into 100 mL aqueous solution (0.03% w/v TPGS solution) while stirring (800 rpm). The
4 acetone was removed completely by stirring overnight at room temperature. Finally, the NPs were
5 obtained through centrifugal separation at 20,000 rpm for 15 min at 4 °C, and washed three times
6 with deionized water to remove the excess TPGS emulsifier and free DTX. The precipitate was
7 re-suspended and placed in a -80 °C refrigerator overnight. The frozen suspension was lyophilized to
8 get the NPs powder. The fluorescent coumarin-6-loaded NPS was prepared through the same
9 procedure except that 1 mg of coumarin-6 was used in the reaction instead of 10 mg DTX.

10 *2.5 Characterization of drug-loaded NPs*

11 *2.5.1 Drug loading and encapsulation efficiency*

12 The drug loading content (LC) and drug encapsulation efficiency (EE) of the drug-loaded NPs
13 were evaluated by high performance liquid chromatography (HPLC) according to previously
14 reported methods.³⁹ Briefly, DTX-loaded nanoparticles (5 mg) were dissolved in 1 mL
15 dichloromethane while stirring. Then the solution was poured into 5 ml of solvent mixture
16 (chromatography grade acetonitrile and deionized water 50:50, v/v). The dichloromethane was
17 evaporated by passing a nitrogen stream through the solution for about 15 min. Subsequently, the
18 solution was filtered and the DTX content was determined at absorbance 227 nm by HPLC (LC 1200,
19 Agilent Technologies, Santa Clara, CA, USA) equipped with a reverse-phase C-18 column (150 mm
20 × 46 mm, GL Sciences Inc., Tokyo, Japan). The mobile phase consisted of deionized water and
21 acetonitrile (50:50, v/v) at the constant flow rate of 1.0 mL/min. The value of LC and EE were
22 determined by the following formulae, respectively.

$$\text{LC (\%)}_{\text{DTX}} = \frac{\text{Weight of DTX in the NPs}}{\text{Weight of the NPs}} \times 100\%$$
$$\text{EE (\%)}_{\text{DTX}} = \frac{\text{Weight of DTX in the NPs}}{\text{Weight of the feeding DTX}} \times 100\%$$

1 2.5.2 Morphological analysis of NPs

2 The surface morphology of DTX-loaded NPs was investigated using field emission scanning
3 electron microscopy (FESEM) and transmission electron microscopy (TEM). The NPs power was
4 suspended by deionized water, and then the solution was dropped onto a piece of monocrystalline
5 silicon and was dried in a vacuum drying oven at room temperature overnight. The prepared samples
6 were coated with platinum layer by JFC-1300 automatic fine platinum coater (JEOL, Tokyo, Japan).
7 After sample preparation, the NPs were analyzed by field emission scanning electron microscopy
8 (FESEM, JEOL JSM-6301F, Tokyo, Japan). To further observe the morphology of NPs,
9 transmission electron microscopy (TEM, TecnaiG2 20, FEI Company, Hillsboro, Oregon, USA) was
10 used to scan the NPs. The solution of NPs power was dropped onto a copper grid coated with a
11 carbon membrane and dried at room temperature before characterization.

12 2.5.3 Size and zeta potential

13 The particle size and zeta potential of the NPs were examined by Malvern Mastersizer 2000
14 (Zetasizer Nano ZS90, Malvern Instruments Ltd., UK). The freshly prepared nanoparticles were
15 appropriately diluted before measurement. All measurements were performed in triplicate.

16 2.5.4 Differential scanning calorimetry (DSC) analysis

17 DSC analysis was used to characterize the physical status of DTX in amphiphilic copolymer NPs,
18 using a differential scanning calorimetry (STA449F3, Netzsch, Germany). The NPs were purged
19 with dry nitrogen at a flow rate of 20 mL/min and were heated from room temperature to 200 °C at a
20 rate of 10 °C/min.

1 2.5.5 *In vitro* drug release

2 In vitro DTX release from drug-loaded NPs was performed as described previously.³ In brief, 5
3 mg of DTX-loaded NPs powder was suspended in 1 mL release buffer (PBS, containing 0.1% Tween
4 80, pH=7.4 or pH=5.0) and transferred into a dialysis membrane bag (Spectra Por®, MWCO=3,500,
5 Spectrum, Houston, TX, USA). Then the bags were immersed into 15 mL release buffer inside a
6 centrifuge tube and incubated in a shaking bath at 37 °C, at 200 rpm. The release buffer was replaced
7 with fresh release buffer every day. The released DTX was extracted from the collected release
8 buffer by DCM, and the DCM solution of DTX was then placed into an evacuated container. After
9 evaporation of DCM, the solid DTX residue was dissolved in methanol (HPLC grade) and analyzed
10 by HPLC as described above. In this manner, the cumulative DTX amount released over 14 days was
11 determined.

12 2.6 *Reactive oxygen species (ROS) assay*

13 In order to measure the amount of singlet oxygen (¹O₂) generated by TAPP-PLA-*b*-TPGS,
14 1,3-diphenylisobenzofuran (DPBF) was used as the singlet oxygen scavenger.¹¹ The
15 TAPP-PLA-*b*-TPGS or PLA-*b*-TPGS was first dissolved in a small amount of DMSO. Then the
16 solution was added into methanol to form a polymer-methanol solution. The DPBF scavenger
17 solution in methanol was also prepared by the same procedure. The two solutions were then mixed to
18 get a polymer concentration of 100 µg/ml. The mixtures were illuminated by light of 660±10 nm
19 wavelength using LEDs from Yabo Scientific and Technical Corporation (Shenzhen, China). The
20 mean fluence rate of the device was 18.49 mW/cm². The decreased absorption rate of DPBF was
21 measured by the microplate reader (Epoch, BioTek Instruments Inc., Highland Park, USA), using the
22 absorption band at 410 nm.

1 2.7 Cellular uptake of Coumarin 6-loaded NPs

2 In this study, coumarin-6 can be used as the fluorescent standard as it shows strong green
3 fluorescence (Ex/Em = 430/485 nm). For qualitative analysis, cells were seeded in 12-well plates
4 containing cover glasses (diameter 18 mm) overnight. Then the cells were cultured in the DMEM
5 containing 100 µg/mL coumarin-6 loaded TAPP-PLA-*b*-TPGS NPs. After 30 min, the cover glass
6 was washed with PBS. The cells were fixed on the cover glass with 4% paraformaldehyde for 20 min
7 and the nuclei were stained with DAPI. The samples were observed by laser scanning confocal
8 microscope (CLSM, Olympus Fluoview FV-1000, Tokyo, Japan).

9 2.8 Immuno cytochemical staining

10 Cells were cultured in 12-well plates with cover glass (diameter 18 mm) and fixed in 95% air
11 humidified atmosphere containing 5% CO₂ at 37 °C for 24 h to allow attachment. DTX/DTX-loaded
12 NPs/drug-free NPs were added into the wells at 100 ng/mL drug concentration for 30 min to allow
13 cellular uptake. Then the cells were allowed to grow in DMEM with 10% FBS for 6 h. Cells were
14 fixed and stained with a primary antibody against α-tubulin at a dilution of 1:100 at 4 °C overnight.
15 A FITC-conjugated goat anti-rabbit IgG was used to combine the α-tubulin antibody. Cell nucleus
16 were stained with DAPI and observed by laser scanning confocal microscope as described above.

17 2.9 Cytotoxicity of DTX-loaded NPs

18 Cells were seeded in 96-well plates at a density of 1×10⁴ cells/well and incubated overnight.
19 Then DTX-loaded or drug-free TAPP-PLA-*b*-TPGS nanoparticle suspension and commercial
20 Taxotere[®] at equivalent docetaxel concentrations 0.25, 2.5, 12.5 and 25 µg/mL were used to culture
21 the cells for 24, 48 and 72 h. At a specific time, the medium was replaced with DMEM containing
22 MTT (5 mg/mL) and cells were then incubated for an additional 4 h. After that, MTT was removed

1 and DMSO was added to dissolve the formazan crystals. Absorbance was measured at 570 nm using
2 the microplate reader as above. Untreated cells were taken as control with 100% viability. The IC₅₀
3 value, the drug concentration at which there is 50% inhibition of cell growth compared to the control
4 sample, was calculated by curve fitting of the cell viability data.

5 *2.10 Phototoxicity of drug-free and DTX-loaded NPs mediated PDT*

6 In order to estimate the copolymer mediated PDT effect, cells were seeded into 96-well plates at
7 a density of 3×10^4 cells/well and incubated overnight. Then, the normal medium was replaced with
8 the medium containing various concentrations of drug-free or drug-loaded NPs, and the cells were
9 incubated at 37 °C for an additional 24 h. The cells were then washed with PBS three times.
10 Thereafter, the cells were exposed to light emitted by the LED, for three different irradiation times of
11 5 min, 10 min and 15 min. Then the MTT assay was performed as described earlier. When the
12 photosensitizing NPs were added into the medium, all the procedures were conducted in subdued
13 light. IC₅₀ was calculated in the same manner as for the cytotoxicity determination of DTX-loaded
14 NPs described above.

15 *2.11 Statistical analysis*

16 All experiments were repeated at least three times unless otherwise stated. Comparisons were
17 performed using a two-tailed paired Student's t test, and probability (*p*) less than 0.05 was considered
18 statistically significant.

19 **3. Results and discussion**

20 *3.1 Synthesis and characterization of star-shaped copolymers*

21 The synthesis procedure of star-shaped TAPP-PLA-*b*-TPGS is shown in scheme 1. The first
22 step is the preparation of the linear amphiphilic copolymer of PLA-*b*-TPGS by the ring-opening

1 polymerization of D,L-lactide (LA) with TPGS as the initiator and Sn(Oct)₂ as the bulk catalyst, at
2 150 °C. Then, the carboxylated linear polymer of TPGS-*b*-PLA-COOH was conjugated to TAPP
3 through the reaction between amino groups of TAPP and carboxyl groups of TPGS-*b*-PLA-COOH,
4 to form the 4-armed amphiphilic copolymer TAPP-PLA-*b*-TPGS.

5 In order to characterize the formation of the copolymers, ¹H NMR was used and the spectrum is
6 shown in Fig. 1. The characteristic resonances of both TPGS ($\delta\text{H}^{\text{a}} = 3.65$ ppm, TPGS repeating unit:
7 - $\text{CH}_2\text{CH}_2\text{O}$ -) and PLA ($\delta\text{H}^{\text{b}} = 1.62$ ppm, LA repeating unit: - CHCH_3 ; $\delta\text{H}^{\text{c}} = 5.21$ ppm, LA repeating
8 unit: - CHCH_3) were observed, as seen in Fig. 1A, in accordance with those reported by Zeng and
9 co-workers,[21] indicating the successful synthesis of the linear polymer PLA-*b*-TPGS. The
10 structure of star-shaped copolymer of TAPP-LA-*b*-TPGS was confirmed by characteristic peak
11 signals of TAPP moieties ($\delta\text{H}^{\text{d}} = 8.90$ ppm, $\delta\text{H}^{\text{e}} = 7.98$ ppm, $\delta\text{H}^{\text{f}} = 8.23$ ppm) in Fig. 1B, which
12 could not be observed in the ¹H NMR spectrum of the linear PLA-*b*-TPGS, and these results are
13 similar to the study reported by Zhang et al.³⁵ These spectra indicate that the linear polymer
14 PLA-*b*-TPGS and the star-shaped polymer TAPP-PLA-*b*-TPGS are successfully synthesized. The
15 molecular weights (M_n) of the copolymer TAPP-PLA-*b*-TPGS were measured by ¹H NMR and GPC,
16 respectively. The M_n estimated from ¹H NMR spectrum ($M_n = 41,360$) is larger than that from GPC
17 ($M_n = 35,780$). This could be attributed to the fact that molecular weight estimation by GPC analysis
18 uses the linear polymer as calibration, however the star-shaped copolymer TAPP-PLA-*b*-TPGS has a
19 smaller hydrodynamic volume than the linear polymer with similar molecular weight and does not
20 expand much in solution. Similar results were reported in our previous study.^{21,39} Furthermore, the
21 polydispersity index (PDI, M_w/M_n) of the copolymer is 1.24, which is rather narrow.

22 *3.2 Preparation and characterization of NPs*

1 The commonly used chemotherapeutic medication DTX was encapsulated into the polymeric NPs
2 by a modified nanoprecipitation technique using acetone as the solvent of choice. This method was
3 used for the encapsulation as it is reported to perform well as a mild, facile, and low energy process
4 for drug encapsulation of polymeric NPs.⁴⁰ As shown in Fig. 2A, the DTX was encapsulated in the
5 core of TAPP-PLA-*b*-TPGS NPs without any chemical modification through the nanoprecipitation
6 elaboration approach. Acetone was used to dissolve the polymers and DTX to form a homogenous
7 and clear solution. Then, the acetone solution was slowly injected into aqueous TPGS solution
8 while stirring. In the water, stable nanoparticles were spontaneously formed, with the hydrophobic
9 PLA at the core surrounding water-insoluble DTX, and hydrophilic TPGS segment as the outer
10 shell.⁴¹ Finally, in order to obtain stable DTX-loaded NPs, the reaction mixture was stirred
11 overnight to evaporate the organic solvent acetone, followed by centrifugation and lyophilization to
12 yield the NPs as loose powder.

13 3.2.1. *Size, zeta potential, morphology and drug encapsulation efficiency*

14 As particle size and surface properties of the NPs play an important role in cellular uptake, drug
15 release, in vivo pharmacokinetics and biodistribution, the size and size distribution of the
16 DTX-loaded NPs were estimated by dynamic light scattering (DLS) experiments and the results are
17 displayed in Table 1. It has been previously reported that 100~200 nm sized NPs have higher cellular
18 uptake efficiency.⁴² The mean hydrodynamic sizes of DTX-loaded PLA-*b*-TPGS and DTX-loaded
19 TAPP-PLA-*b*-TPGS NPs were found to be about 100~130 nm in diameter, which falls in the
20 excellent size range for increasing the cellular uptake, enhanced permeability and retention
21 (EPR)^{12,43} effect of the drug. The TAPP-PLA-*b*-TPGS NPs had an average size of around 127 nm,
22 and also displayed a relatively narrow size distribution (PDI=0.159), which makes them attractive

1 choices in drug delivery systems. The size distribution data of the DTX-loaded TAPP-PLA-*b*-TPGS
2 NPs is shown in Fig. 2B.

3 The zeta potentials of DTX-loaded TAPP-PLA-*b*-TPGS NPs and DTX-loaded PLA-*b*-TPGS
4 were -9.09 mV and -6.06 mV, respectively, which was appropriate for NPs dispersibility and cell
5 accessibility.¹³ Compared to the DTX-loaded PLA-*b*-TPGS NPs, the DTX-loaded
6 TAPP-PLA-*b*-TPGS showed higher drug loading content (8.65%) and encapsulation efficiency
7 (95.14%) (Table 1). There are two reasons that may account for this phenomenon. At first, the
8 star-shaped core region PLA would have strong binding affinity with hydrophobic DTX molecule.
9 Then, many arms of star-shaped TAPP-PLA-*b*-TPGS could interact with DTX molecule from
10 various directions, which show higher efficiency than the linear PLA-*b*-TPGS.

11 FESEM and TEM experiments were used to characterize the morphology of the
12 TAPP-PLA-*b*-TPGS NPs. Fig. 2C and Fig. 2D present the FESEM and TEM data of the NPs,
13 respectively. From the images, the nearly-spherical shaped NPs can be clearly recognized, with a
14 mean size of nearly 100 nm. The diameter of NPs decreases somewhat when they are in a dry state,
15 thus the size obtained from TEM and FESEM measurements is smaller than that from DLS
16 experiments.

17 3.2.2 Differential scanning calorimetry (DSC)

18 In order to investigate the physical state of docetaxel in DTX-loaded TAPP-PLA-*b*-TPGS and
19 PLA-*b*-TPGS NPs, differential scanning calorimetry (DSC) was conducted. DSC is also helpful in
20 determining whether the drug release occurs from the inner or outer region of the NPs. As shown in
21 Fig. 3, the melting endothermic peak of pure docetaxel occurred at 171 °C. However, there is no such
22 peak observed in either DTX-loaded TAPP-PLA-*b*-TPGS NPs or DTX-loaded PLA-*b*-TPGS NPs.

1 This result allows us to conclude that the physical state of docetaxel in the NPs could be a disordered
2 crystalline phase or a solid solution state. Similar results were reported in our previous study as
3 well.³

4 3.2.3 *In vitro drug release*

5 To examine the drug release behavior in vitro, the DTX-loaded NPs were suspended in two
6 separate PBS solutions with different pH (7.4 and 5.0), both containing 0.1% w/v Tween 80 which
7 serves the purpose of increasing the solubility of DTX in the buffer solution and preventing the drug
8 from adhering to the tube wall. The results of the drug release from the DTX-loaded
9 TAPP-PLA-*b*-TPGS NPs in the first 14 days are shown in Fig. 4. In the first 7 days, the total drug
10 released from the TAPP-PLA-*b*-TPGS, in acidic condition (pH 5.0), reached to 60.09% of the
11 encapsulated drugs, and the value reached to 77.42% of the encapsulated drugs after 14 days. These
12 drug release values are higher than the results in simulated physiological condition with pH 7.4
13 (45.67% and 60.15% in 7 and 14 days, respectively). The results indicated that the drug release from
14 star-shaped polymer TAPP-PLA-*b*-TPGS NPs in acidic condition is faster than that in normal neutral
15 pH condition. The accelerated hydrolysis of the ester bonds linking the arms and core of the structure,
16 and the ester bonds in the PLA under acidic conditions, may contribute to the enhanced drug release
17 at lower pH.⁴¹ The intracellular pH of tumors is reported to be lower than in healthy tissues and
18 endosomal pH may range from 4.5 to 6.5.¹³ Therefore, this pH dependent release behavior of
19 DTX-loaded TAPP-PLA-*b*-TPGS NPs is suitable for pH-triggered drug delivery in cancer therapy.

20 3.3 *Cellular uptake of coumarin 6-loaded NPs*

21 It has been shown that internalization and sustained retention of the NPs by cancer cells can
22 have a significant impact on the therapeutic effects of the drug-loaded NPs.⁴⁴ Coumarin 6-loaded

1 NPs were used to investigate the cellular uptake efficiency of the NPs. The HeLa cells were
2 cultured in 100 $\mu\text{g}/\text{mL}$ Coumarin 6-loaded TAPP-PLA-*b*-TPGS NPs suspension for 30 minutes,
3 and then the cells were observed by CLSM after sample preparation. The images shown in Fig. 5
4 were obtained from DAPI channel (blue), FITC channel (green) and the overlay of the two
5 channels. As shown in Fig. 5, the HeLa cells' cytoplasm emitted considerable green fluorescence,
6 which indicated that the entire amount of coumarin 6-loaded TAPP-PLA-*b*-TPGS NPs had been
7 internalized into the HeLa cells as quickly as in 30 minutes. This could be attributed to the small
8 size of the TAPP-PLA-*b*-TPGS NPs, as the particle size plays a major role in the cellular uptake of
9 biodegradable polymeric NPs. Thus, the star-shaped copolymer of TAPP-PLA-*b*-TPGS may have
10 an excellent performance in the drug-delivery system.

11 3.4 *Effects of paclitaxel on microtubules in HeLa cells*

12 The mechanism of DTX is that the drug stabilizes microtubules and inhibits the
13 depolymerization of microtubules during mitosis, thus resulting in cell death.⁴⁵ In this assay,
14 anti- α -tubulin primary antibody and FITC-conjugated secondary antibody were used to determine
15 whether the DTX released from the NPs still maintained its bioactivity. In order to ensure that the
16 effects of DTX on microtubules came from the NPs internalized by the cells rather than released
17 from NPs in the medium, the HeLa cells were incubated with the DTX loaded NPs at 100 ng/mL
18 equivalent DTX concentration for just 30 min. Then the cells were washed and incubated in normal
19 DMEM medium for 6 h to allow the drug inside the cells to work, and the immunofluorescence
20 stained microtubules were observed by CLSM. The images are shown in the Fig. 6. The
21 microtubules of the drug-free TAPP-PLA-*b*-TPGS NPs incubated cancer cells show a clear and
22 organized distribution which is the same as the control. Thus, it is evident that the blank NPs had no

1 effect on the distribution of microtubules. However, the cells incubated with DTX-loaded
2 TAPP-PLA-*b*-TPGS NPs showed bundled microtubules, which is similar to the results obtained with
3 Taxotere[®]. On the one hand, these results are similar to cellular uptake of coumarin 6-loaded NPs
4 experiment, that DTX-loaded TAPP-PLA-*b*-TPGS NPs were entrapped in the cancer cells within a
5 short period of time (30 min). On the other hand, these results show that DTX can be released from
6 the NPs and presented similar pharmaceutical effects as the Taxotere[®] at relatively low concentration.
7 Thus, the star-shaped copolymer of TAPP-PLA-*b*-TPGS has the potential to provide excellent
8 therapeutic effects of the drug-loaded NPs.

9 3.5 Reactive oxygen species (ROS) assay

10 In PDT, the cells are killed mostly due to the singlet oxygen (¹O₂) species generated from the
11 photosensitizer when irradiated by light of specific wavelengths.^{6,10} To investigate the singlet oxygen
12 (¹O₂) generation of TAPP-PLA-*b*-TPG, we used 1,3-diphenylisobenzofuran (DPBF) as the scavenger
13 to react with singlet oxygen (¹O₂) and trap it. The decreased absorption value of DPBF is positively
14 correlated to the ¹O₂ quantum yields. The singlet oxygen (¹O₂) generation profile is shown in Fig. 7.
15 The absorbance of DPBF containing PLA-*b*-TPGS was almost unchanged under several different
16 irradiation times. However, with increasing irradiation time, the absorbance of DPBF containing
17 TAPP-PLA-*b*-TPGS decreased significantly. Therefore, TAPP-PLA-*b*-TPGS was able to exhibit
18 efficient singlet oxygen (¹O₂) generation, which was the most important factor for potential
19 photosensitizer. This property of TAPP-PLA-*b*-TPGS is likely attributed to the porphyrin core of
20 star-shaped polymer, which helps to promote the singlet oxygen (¹O₂) generation.

21 3.6 Cytotoxicity and phototoxicity of TAPP-PLA-*b*-TPGS

22 In order to evaluate the cytotoxicity of drug-free TAPP-PLA-*b*-TPGS NPs, DTX-loaded

1 TAPP-PLA-*b*-TPGS NPs and commercial Taxotere[®], the HeLa cells were used in the MTT assay in
2 the absence of light. Figures 8A-C show the cells viability after culturing with NPs at equivalent
3 DTX concentrations of 0.25, 2.5, 12.5 and 25 $\mu\text{g}/\text{mL}$ for 12h, 24h, and 48h. In the earlier
4 microtubule polymerization assay, we have demonstrated that the star-shaped amphiphilic copolymer
5 TAPP-PLA-*b*-TAPP had no effect on the microtubule protein. Furthermore, the polymer also did not
6 display any cytotoxicity at various concentrations and during different time periods in this MTT
7 assay. These results further indicate that the star-shaped copolymer of TAPP-PLA-*b*-TPGS would
8 make a good biocompatible and non-toxic drug delivery system. On the other hand, the drug-loaded
9 TAPP-PLA-*b*-TPGS NPs had an advantage in decreasing the HeLa cell viability, as the cell viability
10 reached as low as 19.5% at equivalent DTX concentration of 25 $\mu\text{g}/\text{mL}$ after 72 h. Also, the
11 cytotoxicity of the DTX-loaded TAPP-PLA-*b*-TPGS NPs is likely to increase by prolonging the
12 culture time and increasing the NPs concentration, thus exhibiting a dose-dependent and
13 time-dependent effect. Although the DTX-loaded NPs and the Taxotere[®] showed similar effects on
14 the HeLa cells after 24 h (Fig. 8A), the DTX-loaded TAPP-PLA-*b*-TPGS NPs showed significantly
15 higher cytotoxicity than the commercial Taxotere[®] after 48 h and 72 h cell incubation (Fig. 8B and
16 Fig. 8C). This trend was also observed in the IC_{50} values. The IC_{50} values of HeLa cells after 48 and
17 72 h incubation with the DTX-loaded TAPP-PLA-*b*-TPGS NPs were much smaller than the values
18 obtained with Taxotere[®] (Table 2). This may be due to the fact that the TAPP-PLA-*b*-TPGS NPs are
19 able to increase the cellular uptake and the drug-loaded NPs within the cells can then release the drug
20 to the cytoplasm.

21 To investigate phototoxicity of the drug-free TAPP-PLA-*b*-TPGS NPs and DTX-loaded
22 TAPP-PLA-TPGS NPs, the viability of the HeLa cells were assessed after exposing them to light for

1 5, 10 and 15 min followed by culturing for 24 h. As shown in the Fig. 8 D-F, the drug-free
2 TAPP-PLA-*b*-TGPS NPs destroyed the HeLa cells at equivalent DTX concentration more than 12.5
3 $\mu\text{g}/\text{mL}$ after irradiating for 10 min or 15 min, while they did not show any cytotoxicity towards the
4 HeLa cells in dark, based on the previous experiment. The DTX-loaded TAPP-PLA-*b*-TPGS NPs
5 killed only 48.8% of HeLa cells at the highest concentration 25 $\mu\text{g}/\text{mL}$ in dark after culturing 24 h,
6 while the drug-loaded NPs killed 71.7% and 78.8% of HeLa cells at the same concentration and
7 same culturing time after 10 min and 15 min irradiation, respectively (Fig. 7E and Fig. 7F). Also, the
8 DTX-loaded TAPP-PLA-*b*-TPGS exerted higher cytotoxicity on HeLa cells than the commercial
9 Taxotere[®], although there were no significant differences between drug-loaded NPs and Taxotere[®]
10 after culturing for 24h in dark (Fig. 7A). This trend could be quantitatively demonstrated in terms of
11 IC_{50} values. The values of IC_{50} were 5.04 $\mu\text{g}/\text{mL}$ and 1.93 $\mu\text{g}/\text{mL}$ for irradiation time 10 min and 15
12 min, respectively, after culturing 24 h. These values are smaller than the IC_{50} value of 23.06 $\mu\text{g}/\text{mL}$
13 in dark, at the same culturing time. These results indicate that PDT of TAPP-PLA-*b*-TPGS may
14 promote synergistic effects with DTX. There may be three reasons that account for the enhancement
15 of cytotoxicity. First, the excellent size of the NPs and the zeta potential likely contributed to the
16 increased cellular uptake. Also, the TPGS is possibly able to prevent the P-glycoprotein on cell
17 membrane from pumping DTX out of the cytoplasm.^{46,47} Second, the photochemical internalization
18 (PCI) effect is an important factor.⁴⁸ The DTX-loaded NPs are endocytosed and some of them are
19 entrapped into the endosome and lysosome. In combination with exposure to light, reactive oxygen
20 species generating from photosensitizers could breakdown the endosomal and lysosomal membranes
21 to release the drug into the cytoplasm. Third, the ROS are generated by TAPP-PLA-*b*-TPGS after
22 irradiation, which then kills the cells by destroying the organelle.⁹

1

2 **4. Conclusions**

3 In this work, a new type of four-armed star-shaped porphyrin-cored PLA-*b*-TPGS copolymer
4 (TAPP-PLA-*b*-TPGS) has been successfully synthesized for use in drug delivery and PDT
5 applications. The drug-loaded nanoparticles formed through TAPP-PLA-*b*-TPGS encapsulation of
6 DTX showed significantly higher drug loading concentration and drug encapsulation efficiency, and
7 achieved faster drug release in slightly acidic medium. The DTX-loaded TAPP-PLA-*b*-TPGS also
8 showed superior in vitro anticancer performance with HeLa cells than commercial Taxotere[®] and
9 exhibited excellent cytotoxicity towards cervical carcinoma after irradiation. We believe that a
10 synergistic effect exists between PDT and DTX which is responsible for enhanced destruction of
11 HeLa cells, when the multifunctional TAPP-PLA-*b*-TPGS material serves as the drug nanocarriers.
12 Therefore, the star-shaped copolymer TAPP-PLA-*b*-TPGS has potential applications in the
13 development of a new multi-modality treatment approach for cancer.

14

15 **Acknowledgments**

16 This work was supported by the National Natural Science Foundation of China (No. 31270019,
17 51203085), Program for New Century Excellent Talents in University (NCET-11-0275), Guangdong
18 Natural Science Funds for Distinguished Young Scholar (No. 2014A030306036), Scientific and
19 Technological Innovation Bureau of Nanshan District (No. KC2014JSCX0023A), Science,
20 Technology & Innovation Commission of Shenzhen Municipality (No. KQC201105310021A, CYZZ
21 20130320110255352) and Tianjin Municipal Natural Science Foundation (No. 15JCZDJC38300).

22

1 **References**

- 2 1 G. Suneja, M. Bacon, W. J. Small, S. Y. Ryu, H. C. Kitchener and D. K. Gaffney, *Front.*
3 *Oncol.*, 2015, **5**, 14.
- 4 2 J. Ferlay, H. Shin, F. Bray, D. Forman, C. Mathers and D. M. Parkin, *Int. J. cancer*, 2010, **127**,
5 2893–2917.
- 6 3 X. Zeng, W. Tao, L. Mei, L. Huang, C. Tan and S.-S. Feng, *Biomaterials*, 2013, **34**, 6058–
7 6067.
- 8 4 J. Baker, J. Ajani, F. Scotté, D. Winther, M. Martin, M. S. Aapro and G. von Minckwitz, *Eur.*
9 *J. Oncol. Nurs.*, 2009, **13**, 49–59.
- 10 5 Z. Wang, X. Zeng, Y. Ma, J. Liu, X. Tang, Y. Gao, K. Liu, J. Zhang, P. Ming, L. Huang and L.
11 Mei, *J. Biomed. Nanotechnol.*, 2014, **10**, 1509–1519.
- 12 6 D. E. Dolmans, D. Fukumura and R. K. Jain, *Nat. Rev. Cancer*, 2003, **3**, 380–387.
- 13 7 B. W. Henderson and T. J. Dougherty, *Photochem. Photobiol.*, 1992, **55**, 145–157.
- 14 8 T. J. Dougherty, C. J. Gomer, B. W. Henderson, G. Jori, D. Kessel, M. Korbelik, J. Moan and
15 Q. Peng, *J. Natl. Cancer Inst.*, 1998, **90**, 889–905.
- 16 9 S. B. Brown, E. A. Brown and I. Walker, *Lancet Oncol.*, 2004, **5**, 497–508.
- 17 10 C. A. Robertson, D. H. Evans and H. Abrahamse, *J. Photochem. Photobiol. B Biol.*, 2009, **96**,
18 1–8.
- 19 11 C.-L. Peng, M.-J. Shieh, M.-H. Tsai, C.-C. Chang and P.-S. Lai, *Biomaterials*, 2008, **29**,
20 3599–3608.
- 21 12 J. Nicolas, S. Mura, D. Brambilla, N. Mackiewicz and P. Couvreur, *Chem. Soc. Rev.*, 2013, **42**,
22 1147–1235.
- 23 13 B. Daglar, E. Ozgur, M. E. Corman, L. Uzun and G. B. Demirel, *RSC Adv.*, 2014, **4**, 48639–
24 48659.
- 25 14 M.-C. Jones and J.-C. Leroux, *Eur. J. Pharm. Biopharm.*, 1999, **48**, 101–111.
- 26 15 K. S. Soppimath, T. M. Aminabhavi, A. R. Kulkarni and W. E. Rudzinski, *J. Control. Release*,
27 2001, **70**, 1–20.
- 28 16 N. Kamaly, Z. Xiao, P. M. Valencia, A. F. Radovic-Moreno and O. C. Farokhzad, *Chem. Soc.*
29 *Rev.*, 2012, **41**, 2971–3010.

- 1 17 H.-B. Shang, F. Chen, J. Wu, C. Qi, B.-Q. Lu, X. Chen and Y.-J. Zhu, *RSC Adv.*, 2014, **4**,
2 53122–53129.
- 3 18 V. Lassalle and M. L. Ferreira, *Macromol. Biosci.*, 2007, **7**, 767–783.
- 4 19 A. Kumari, S. K. Yadav and S. C. Yadav, *Colloids Surfaces B Biointerfaces*, 2010, **75**, 1–18.
- 5 20 Y. Cheng, S. Deng, P. Chen and R. Ruan, *Front. Chem. China*, 2009, **4**, 259–264.
- 6 21 X. Zeng, W. Tao, Z. Wang, X. Zhang, H. Zhu, Y. Wu, Y. Gao, K. Liu, Y. Jiang, L. Huang, L.
7 Mei and S.-S. Feng, *Part. Part. Syst. Charact.*, 2015, **32**, 112–122.
- 8 22 M. E. Fox, F. C. Szoka and J. M. J. Fréchet, *Acc. Chem. Res.*, 2009, **42**, 1141–1151.
- 9 23 Z. Zhang, S. Tan and S.-S. Feng, *Biomaterials*, 2012, **33**, 4889–4906.
- 10 24 L. Mu and S. S. Feng, *J. Control. Release*, 2002, **80**, 129–144.
- 11 25 L. Mu and S. S. Feng, *J. Control. release*, 2003, **86**, 33–48.
- 12 26 Z. Zhang, L. Mei and S.-S. Feng, *Nanomedicine*, 2012, **7**, 1645–1647.
- 13 27 L. Z. Benet, T. Izumi, Y. Zhang, J. A. Silverman and V. J. Wachter, *J. Control. Release*, 1999,
14 **62**, 25–31.
- 15 28 Y. Liu, L. Huang and F. Liu, *Mol. Pharm.*, 2010, **7**, 863–869.
- 16 29 H. Zhu, H. Chen, X. Zeng, Z. Wang, X. Zhang, Y. Wu, Y. Gao, J. Zhang, K. Liu, R. Liu, L.
17 Cai, L. Mei and S.-S. Feng, *Biomaterials*, 2014, **35**, 2391–2400.
- 18 30 A. A. Barba, A. Dalmoro, M. d'Amore, C. Vascello and G. Lamberti, *J. Mater. Sci.*, 2014, **49**,
19 5160–5170.
- 20 31 C. Vauthier and K. Bouchemal, *Pharm. Res.*, 2009, **26**, 1025–1058.
- 21 32 F. Wang, T. K. Bronich, A. V Kabanov, R. D. Rauh and J. Roovers, *Bioconjug. Chem.*, 2008,
22 **19**, 1423–1429.
- 23 33 O. G. Schramm, G. M. Pavlov, H. P. van Erp, M. A. R. Meier, R. Hoogenboom and U. S.
24 Schubert, *Macromolecules*, 2009, **42**, 1808–1816.
- 25 34 P. Dong, X. Wang, Y. Gu, Y. Wang, Y. Wang, C. Gong, F. Luo, G. Guo, X. Zhao, Y. Wei and
26 Z. Qian, *Colloids Surfaces A Physicochem. Eng. Asp.*, 2010, **358**, 128–134.
- 27 35 L. Zhang, Y. Lin, Y. Zhang, R. Chen, Z. Zhu, W. Wu and X. Jiang, *Macromol. Biosci.*, 2012,
28 **12**, 83–92.

- 1 36 E. D. Sternberg, D. Dolphin and C. Brückner, *Tetrahedron*, 1998, **54**, 4151–4202.
- 2 37 T.-B. Ren, Y. Feng, Z.-H. Zhang, L. Li and Y.-Y. Li, *Soft Matter*, 2011, **7**, 2329.
- 3 38 T. Govender, S. Stolnik, M. C. Garnett, L. Illum and S. S. Davis, *J. Control. Release*, 1999, **57**,
4 171–185.
- 5 39 W. Tao, X. Zeng, T. Liu, Z. Wang, Q. Xiong, C. Ouyang, L. Huang and L. Mei, *Acta*
6 *Biomater.*, 2013, **9**, 8910–8920.
- 7 40 L. Mei, H. Sun, X. Jin, D. Zhu, R. Sun, M. Zhang and C. Song, *Pharm. Res.*, 2007, **24**, 955–
8 962.
- 9 41 J. Zhu, Z. Zhou, C. Yang, D. Kong, Y. Wan and Z. Wang, *J. Biomed. Mater. Res. - Part A*,
10 2011, **97 A**, 498–508.
- 11 42 S. a Kulkarni and S.-S. Feng, *Pharm. Res.*, 2013, **30**, 2512–22.
- 12 43 L. Dai, C.-X. Li, K.-F. Liu, H.-J. Su, B.-Q. Chen, G.-F. Zhang, J. He and J.-D. Lei, *RSC Adv.*,
13 2015, **5**, 15612–15620.
- 14 44 Y. Gong and F. M. Winnik, *Nanoscale*, 2012, **4**, 360.
- 15 45 H.-Y. Hwang, I.-S. Kim, I. C. Kwon and Y.-H. Kim, *J. Control. Release*, 2008, **128**, 23–31.
- 16 46 E.-M. Collnot, C. Baldes, U. F. Schaefer, K. J. Edgar, M. F. Wempe and C.-M. Lehr, *Mol.*
17 *Pharm.*, 2010, **7**, 642–651.
- 18 47 J. Dintaman and J. Silverman, *Pharm. Res.*, 1999, **16**, 1550–1556.
- 19 48 L. Prasmickaite, A. Høgset, P. K. Selbo, B. Ø. Engesæter, M. Hellum and K. Berg, *Br. J.*
20 *Cancer*, 2002, **86**, 652–657.

21

22

23

24

25

26

27

1

2 **Table 1.** Characterization of DTX-loaded nanoparticles

Polymer	Size(nm)	ZP(mV)	PDI	LC(%)	EE(%)
PLA- <i>b</i> -TPGS	108.5 ± 6.83	-6.06 ± 2.15	0.173	7.40	81.41
TAPP-PLA- <i>b</i> -TPGS	127.2 ± 4.31	-9.09 ± 3.46	0.159	8.65	95.14

3 ZP = Zeta potential, PDI = Polydispersity index, LC = Loading content, EE = Encapsulation efficiency, Error bars
4 represent standard deviation (SD) for $n = 3$.

5

6

7 **Table 2.** IC₅₀ values of Taxotere[®] and DTX-loaded TAPP-PCL-*b*-TPGS on HeLa cells after 24, 48,
8 72 h incubation and exposed to 5, 10, 20 min irradiation after 24 h incubation.

Incubation time (h)	IC ₅₀ (µg/mL)				
	Taxotere [®]	DTX-loaded TAPP-PLA- <i>b</i> -TPGS NPs			
		Dark	5 min	10 min	15min
24	24.77 ± 1.63	23.06 ± 1.71	19.25 ± 1.37	5.04 ± 0.52	1.93±0.15
48	12.75 ± 1.52	4.32 ± 0.41	-	-	-
72	10.25 ± 0.98	0.088 ± 0.013	-	-	-

9

10

11

12

13

14

15

16

17

18

19

1 **Figure Captions**

2 **Scheme. 1.** Synthesis of star-shaped copolymer TAPP-PLA-*b*-TPGS.

3 **Fig. 1.** Typical ^1H NMR spectra of copolymers (A) PLA-*b*-TPGS and (B) TAPP-PLA-*b*-TPGS.

4 **Fig. 2.** (A) Schematic diagram of the preparation of the DTX-loaded TAPP-PLA-*b*-TPGS NPs. (B)
5 DLS size distribution of the DTX-loaded TAPP-PLA-*b*-TPGS NPs; (C) FESEM image of the NPs;
6 (D) TEM image of the NPs.

7 **Fig. 3.** DSC analysis thermograms of the pure DTX, the DTX-loaded TAPP-PLA-*b*-TPGS NPs, and
8 the DTX-loaded PLA-*b*-TPGS NPs.

9 **Fig. 4.** *In vitro* drug release profile of DTX-loaded TAPP-PLA-*b*-TPGS NPs at pH 5.0 and pH 7.4.

10 Error bars represent standard deviation (SD) for $n = 3$. $*p < 0.05$ (t-test).

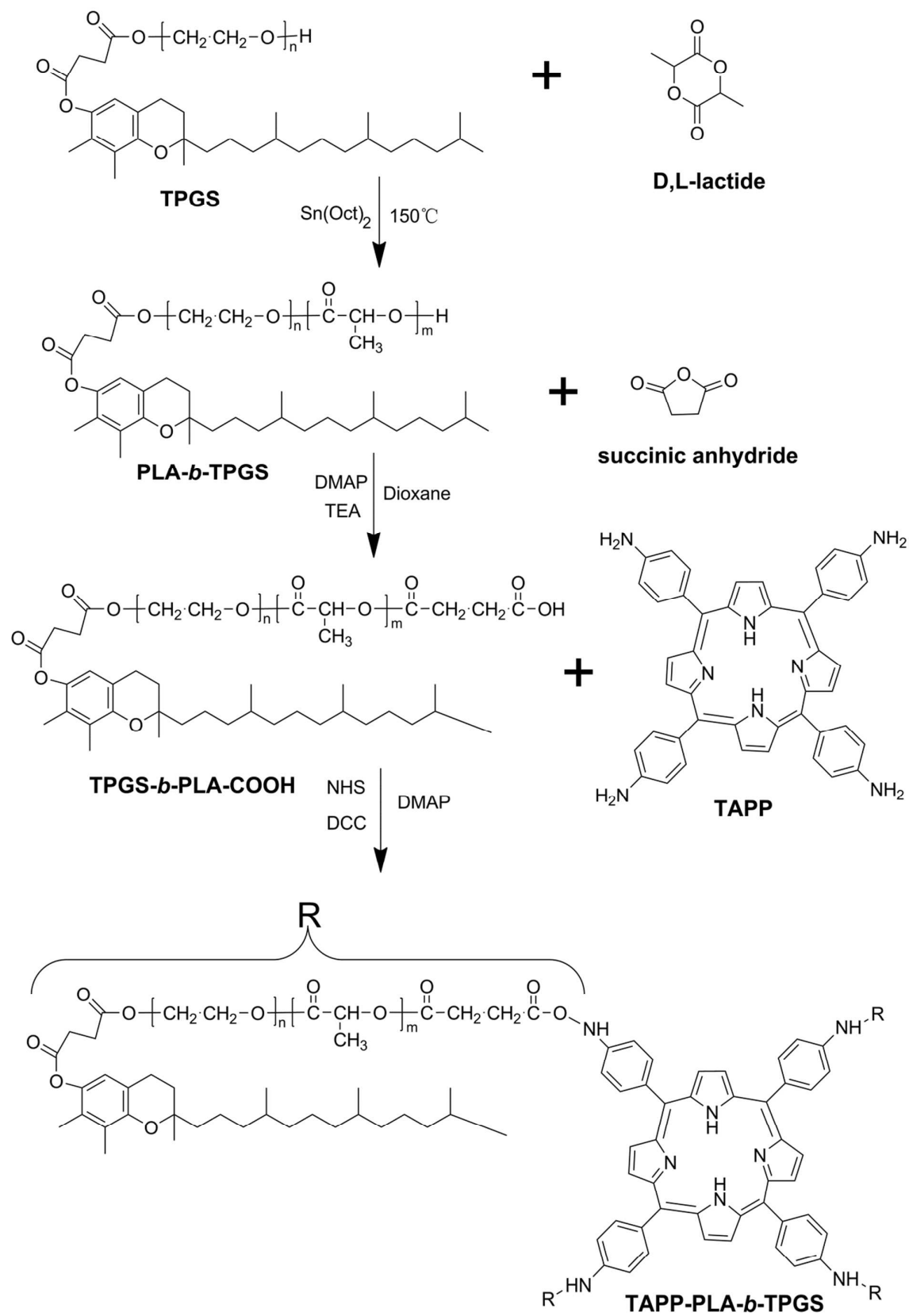
11 **Fig. 5.** Confocal laser scanning microscopy (CLSM) images of HeLa cells after 30 min treated with
12 the Coumarin 6-loaded TAPP-PLA-*b*-TPGS NPs. Coumarin-6 is green and cell nucleus is stained
13 with DAPI (Blue).

14 **Fig. 6.** Confocal laser scanning microscopy (CLSM) images of microtubule in HeLa cells which
15 were incubated with DTX for 30 min, and were cultured with drug-free medium for another 6 h.
16 Cells were stained with anti- α -tubulin antibody to determine the effect of the NPs on cell microtubule
17 organization. Green: α -tubulin; Blue: Nuclear (DAPI).

18 **Fig. 7.** Singlet oxygen generation profile of TAPP-PLA-*b*-TPGS and PLA-*b*-TPGS. Error bars
19 represent standard deviation (SD) for $n = 3$. $***p < 0.001$ (t-test).

20 **Fig.8.** Viability of HeLa cells cultured with the DTX-loaded TAPP-PLA-*b*-TPGS NPs compared
21 with that of Taxotere[®] at the same DTX dose and that of the drug-free TAPP-PLA-*b*-TPGS NPs with
22 the same NPs concentration, in dark: (A) 24 h; (B) 48 h; (C) 72 h. Viability of HeLa cells after 24

1 hour, cultured with the DTX-loaded TAPP-PLA-*b*-TPGS NPs compared with that of Taxotere[®] at the
2 same DTX dose and that of the drug-free TAPP-PLA-*b*-TPGS NPs with the same NPs concentration
3 exposed to different irradiation times: (D) 5 min; (E) 10 min; (F) 15 min. Error bars represent
4 standard deviation (SD) for $n = 3$. * $p < 0.05$; ** $p < 0.01$; *** $p < 0.001$ (t-test).



Scheme 1.

1
2

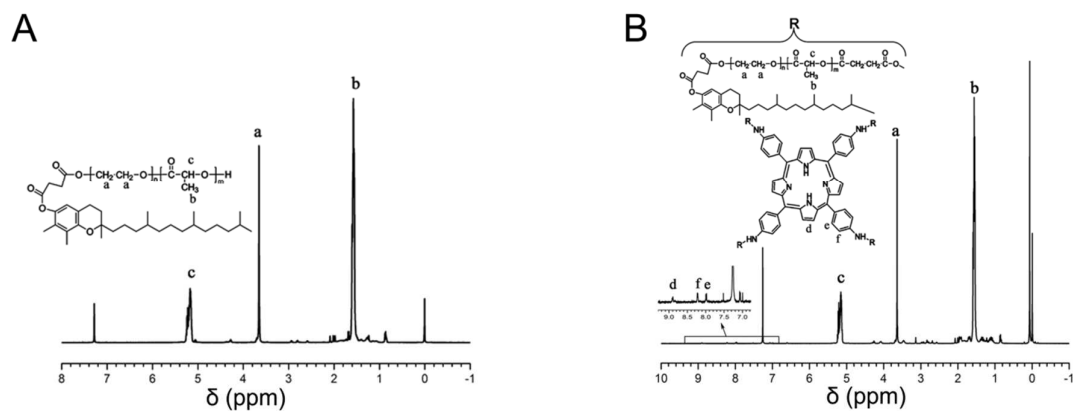
1
2
3

Fig. 1.

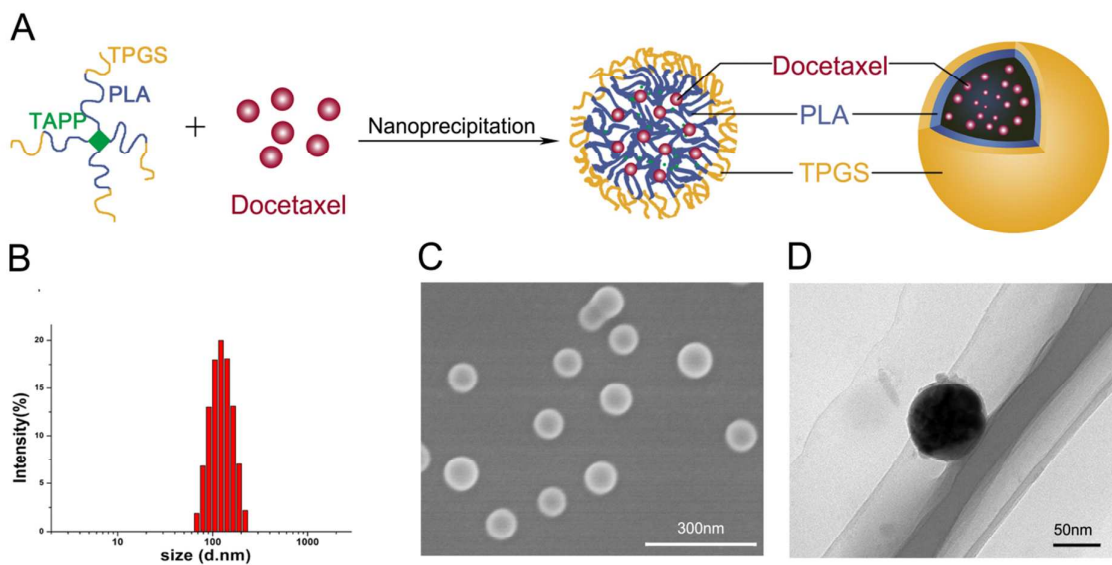
4
5
6

Fig. 2.

7
8
9
10
11
12

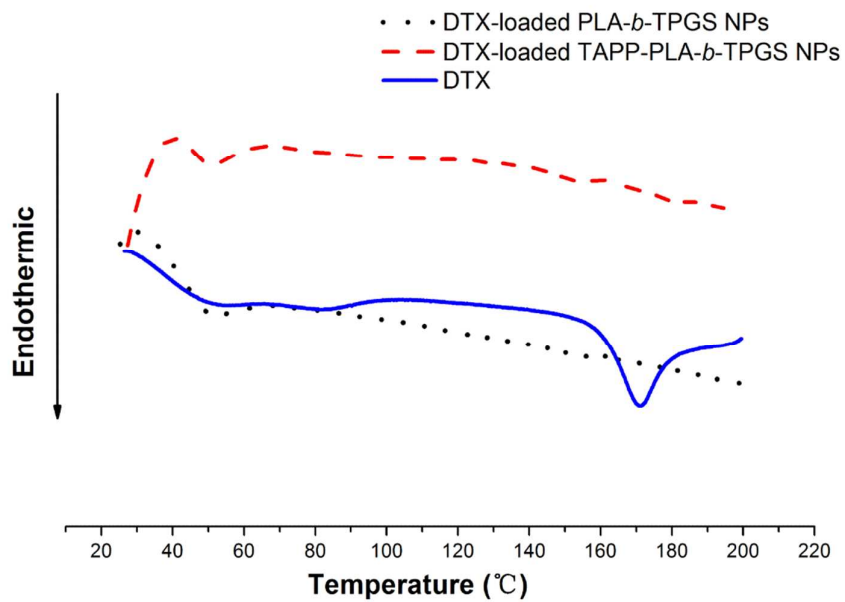


Fig. 3.

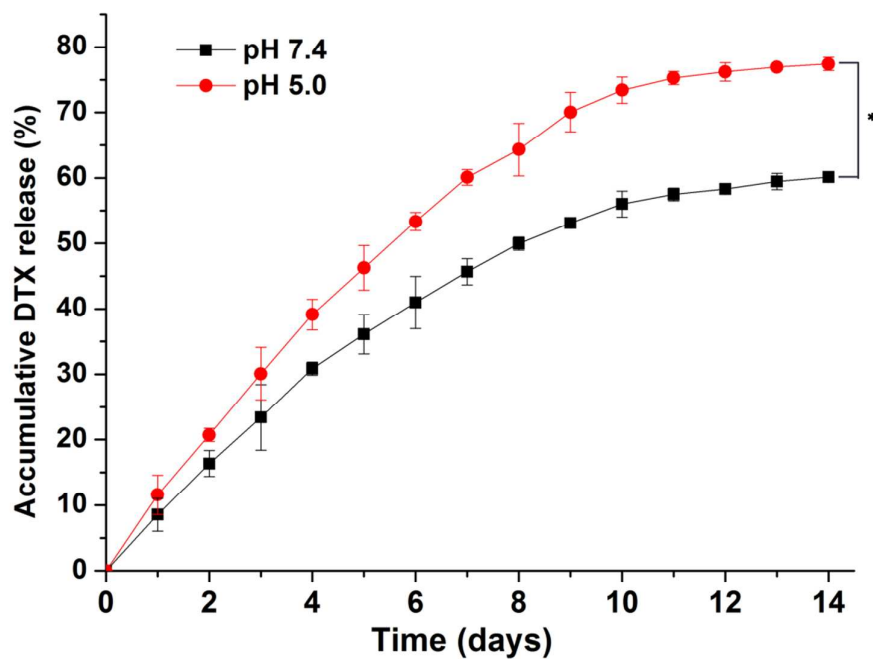


Fig. 4.

1
2
3
4
56
7
8
9

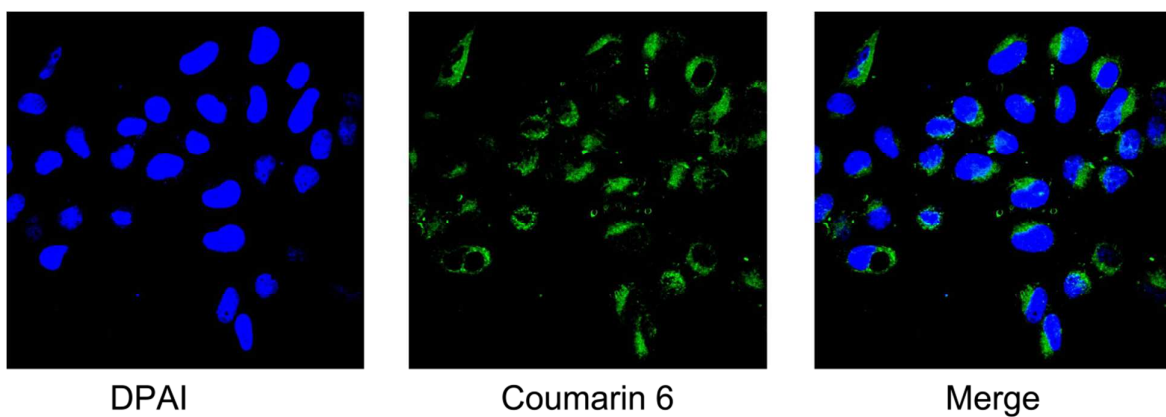


Fig. 5.

1
2
3
4
5
6

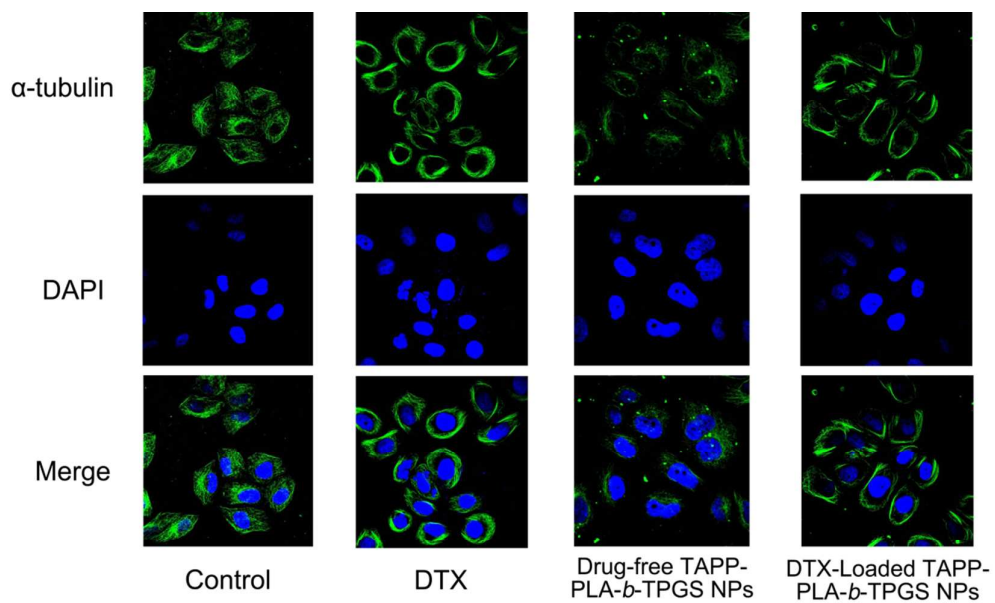


Fig. 6.

7
8
9
10
11
12
13

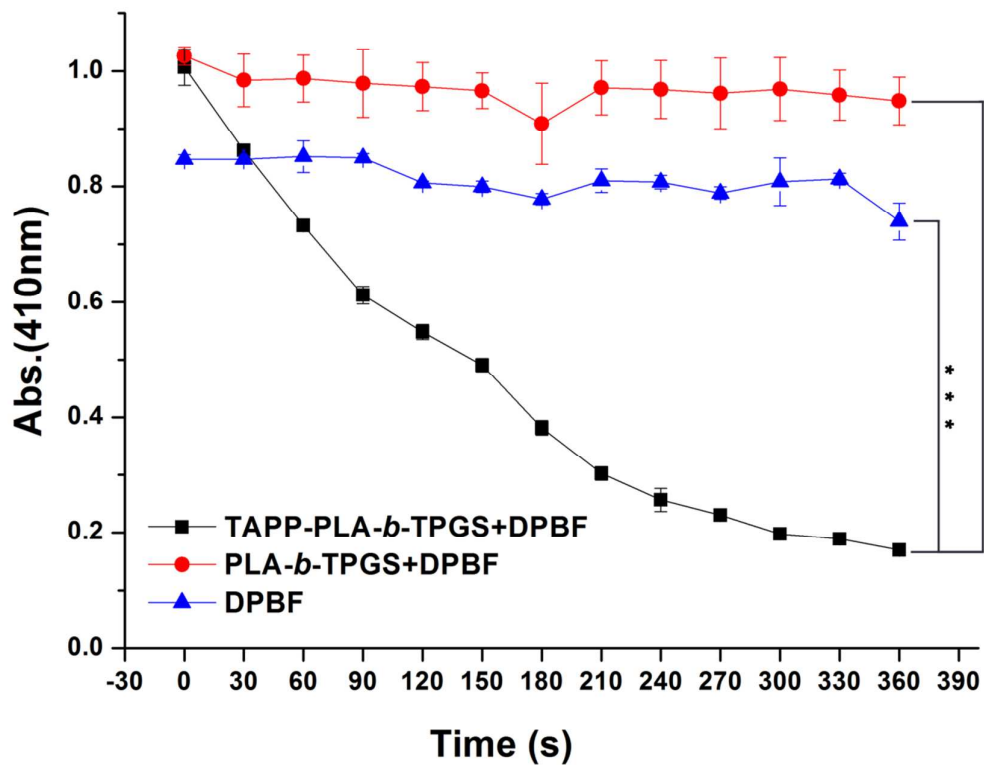


Fig. 7.

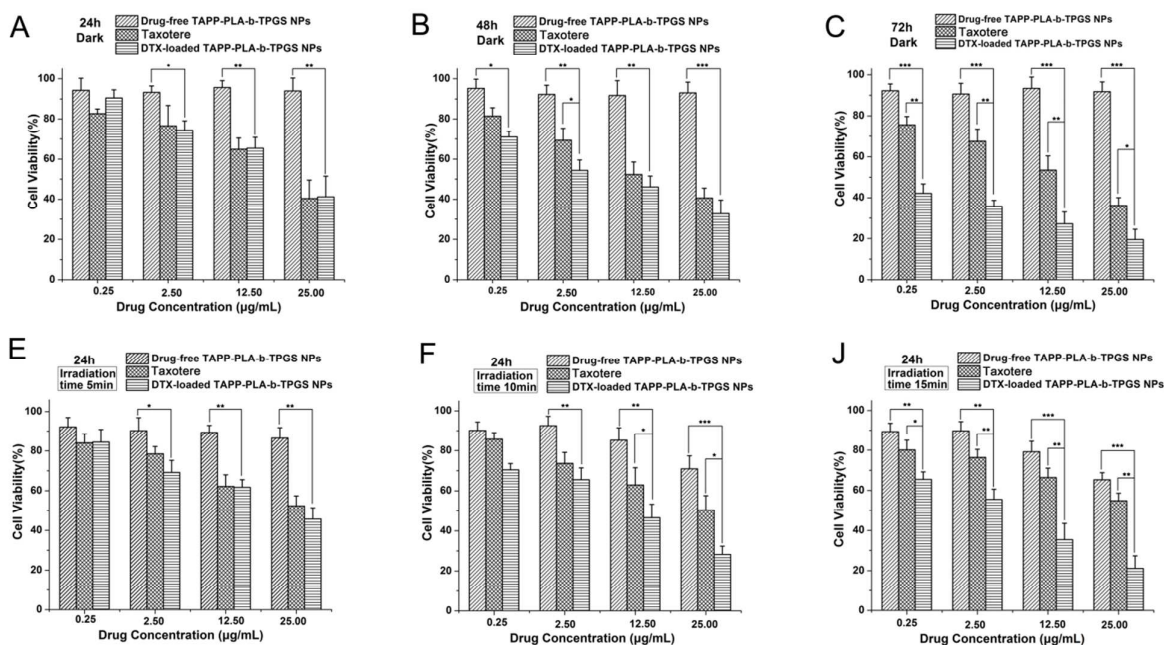


Fig. 8.

1
2
34
5
6